The Peak Control Function and its Applications to Transmission Line Effects in Class D Amplifiers

Dan Tudor VUZA[1], Reinhold FROSCH[2], Helmut KOEBERL[2], Marian VLĂDESCU[3]
[1]*Institute of Mathematics of the Romanian Academy, Bucharest, Romania*
[2]*Freaquent Frosch Electronics GmbH, Graz, Austria*
[3]*CETTI, Politehnica University of Bucharest, Romania*
danvuza@hotmail.com

***Abstract*—Class D amplifiers find new applications in RFID systems, because of their high efficiency. Most textbooks describe the case of a load directly connected to the amplifier. However, in most RFID systems the usage of a transmission line is mandatory and this may introduce some novel effects, in the form of an infinite series of peaks in the system frequency response functions. If not appropriately taken care of, these effects may lead to electromagnetic compatibility problems. The purpose of the paper is to develop the theory of the peak control function, which is conceived as a tool that allows the designer to keep the magnitude of the peaks, and hence their influence on the system, into well defined limits.**

***Index Terms*—Radiofrequency identification, Switching circuits, Power amplifiers, Transmission Lines, Frequency response.**

I. INTRODUCTION

The expanding applications of RFID technology to many areas of industrial and social activities impose to designers the task of looking for high performance systems. Switching amplifiers [1 – 16] represent an attractive solution for RFID [1], [2] and, more generally, for antenna drivers [3] because of their high efficiency in comparison with conventional-type amplifiers. Especially battery-powered handheld readers would benefit from this feature but the same would be true for stationary readers as the concept of a green environment is enforced by many standards and should be the concern of any system designer.

In this paper we shall be concerned with the application of class D amplifiers to RFID readers. There are two types of such amplifiers, voltage-mode and current-mode ([4 – 6], [7] ch. 3 and ch. 2; also [8] for voltage-mode and [9 – 11] for current-mode). Fig. 1A presents the first type. Because of the switching action of the transistors, the voltage V_{MN} imposed on the load circuit of LCR type is a square wave that toggles between V_S and $-V_S$, where V_S is the voltage of the source which powers the amplifier. The LCR circuit is tuned to the switching frequency and is supposed to present a high impedance to the harmonics contained in the voltage square wave. In this way, the current through the load will be mainly composed of a sine wave, the unwanted harmonics in the current being significantly reduced.

Fig. 1B presents a current-mode amplifier. Because of the switching action of the transistors and the property of the RF chokes to maintain an approximately constant current, the current I_{MN} that flows between M and N is a square wave that toggles between I_S and $-I_S$, where I_S is the constant current through one RF choke. Here again the LCR circuit is tuned to the switching frequency and is supposed to present a high impedance to the harmonics contained in the current square wave. Unlike in the voltage-mode case, there must be a low impedance path that can be followed by the latter harmonics. This path is provided by the LC filter connected in parallel with the load, which is also tuned to the switching frequency forcing thus the main Fourier component of the current to pass entirely through the load.

One reason for which class D amplifiers are interesting for RFID is that the load in the form of a series LCR circuit is precisely the equivalent of the tuned antenna circuit that is usually connected to the reader. We see from the above discussion that unlike in conventional amplifiers, where the load is driven with a (more or less) pure sine wave, here the load circuit is supposed to take part in the filtering of the unwanted harmonic components. For the present application the harmonics in the load current are the relevant ones, since the antenna current is the source of the magnetic field that realizes the communication with transponders and hence any

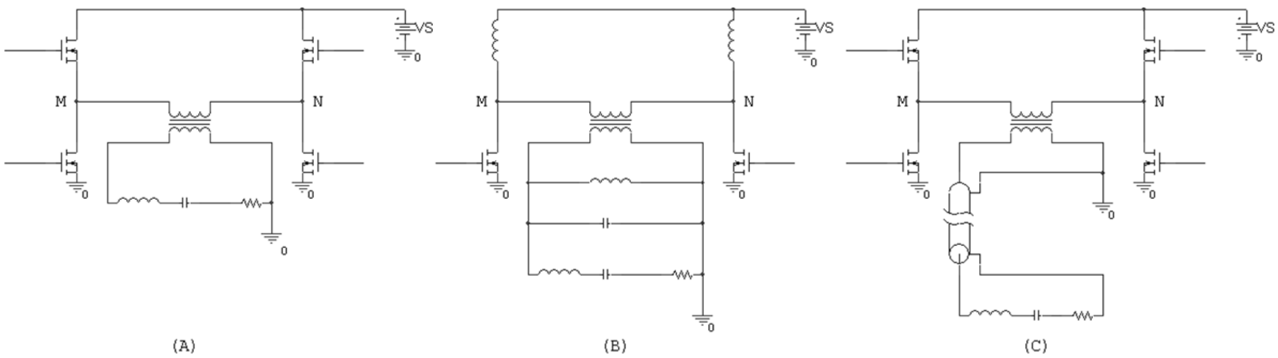

Figure 1. Class D amplifier: voltage-mode (A), current-mode (B) and voltage-mode with transmission line (C).

Digital Object Identifier 10.4316/AECE.2014.03002

uncontrolled harmonics in the current may produce harmonics in the field that are outside of the limits imposed by electromagnetic compatibility standards. The topic of reducing the harmonic content of the output of a switching amplifier is under current research, [12 – 15].

In handheld readers the amplifier and the antenna circuit are located in close proximity on the same physical unit, allowing the designer to have complete control over the nominal antenna parameters that determine in particular the way in which harmonics are filtered. The main feature that distinguishes stationary from handheld systems is the fact that remote placement of the antenna renders mandatory the usage of a transmission line. Because of this there will be some new phenomena arising from the interaction of the line with the antenna and the amplifier that, if overlooked, might lead to an unexpectedly high harmonic content of the antenna current. If we compute the frequency response of the antenna circuit to a harmonic voltage excitation V_{MN} in Fig. 1A, or to a harmonic current excitation I_{MN} in Fig. 1B, we shall see that, in the case usually considered in textbooks (in particular [4 – 6]) when no transmission line is used, there is a rapid increase in attenuation of harmonics in the antenna current as frequency is increased above the switching frequency. Quite differently, when a transmission line is inserted as in Fig. 1C, the corresponding frequency responses for the antenna current may present sharp and rather high peaks at an infinite series of frequencies. If a harmonic in V_{MN}, respectively I_{MN}, happens to be close to any of those frequencies, the effect might be that the harmonic in question is not reduced, but is amplified to such degree that significant field outside of admitted frequency limits is produced, resulting in possible electromagnetic compatibility problems. It will be therefore the system designer's task to ensure this does not happen. The designer should be especially concerned with a design as much as possible immune from this point of view to the variations in the antenna and transmission line characteristics, as in many stationary systems the reader is supposed to work with a multitude of antennas at the user's choice and in some situations, the reader is connected in a multiplexed system which means that at run time it will be connected in turn to several antennas having different characteristics.

One tool that may help the designer in this task is the upper control function defined in the present paper.

It should be noted that in [16] one acknowledges that the presence of a transmission line in a switching amplifier circuit may introduce novel effects and one shows how these effects can be exploited to the benefit of the circuit in a so-called amplifier with multi-harmonic termination. However, this assumes a precise control over the length of the transmission line, which is not the case in this paper.

In a circuit that does not comprise transmission lines, all frequency responses $T(j\omega)$ are rational functions of the frequency variable ω. However, once a transmission line is present, the frequency responses will in general no longer be rational functions but will enclose trigonometric functions of the product ωD, where D is the delay introduced by the line. The presence of such terms makes the frequency responses particularly hard to deal with. For instance, if the design goal is to ensure that upper harmonics are not excessively amplified, the designer should have control over the maxima of $|T(j\omega)|$. In principle one could find the extrema of $|T(j\omega)|$ by solving the equation

$$0=\frac{d}{d\omega}\left|T(j\omega)\right|=\frac{1}{\left|T(j\omega)\right|}\operatorname{Re}\left(\overline{T(j\omega)}\,\frac{d}{d\omega}T(j\omega)\right) \tag{1}$$

where Re (z) and $\bar{z}$ denote respectively the real part and the complex conjugate of a complex number z. However, because of the presence of trigonometric terms, equation (1) is transcendent and not easy to solve exactly.

In the following we shall use the notation $T(j\omega, D)$ for the frequency response of a circuit enclosing one transmission line, emphasizing thus the parametric dependence on D of the response function. We shall be especially interested in the antenna current response to the excitation produced by the amplifier connected at one end of the line (such as V_S in Fig. 3 and I_S in Fig. 4) with the antenna circuit connected at the opposite end. The upper control function $P_T(\omega)$ is defined as the upper bound of $|T(j\omega, D)|$ for all possible delays D. In principle this definition applies to any response function of the mentioned type. Nevertheless, in this paper we shall be concerned with a special subclass of functions $T(j\omega, D)$, which we have called *simply controlled*, for which $P_T(\omega)$ can be computed exactly in terms of the circuit parameters. Since $|T(j\omega, D)| \leq P_T(\omega)$ by the very definition of P_T, we may say that $P_T(\omega)$ prescribes a minimal attenuation at ω to all systems described by the functions $T(j\omega, D)$. Consequently, if the designer has tuned P_T to satisfy, on a domain of frequencies, the attenuation specifications of the application, he may be sure that the system will meet the specifications *irrespective of the length of the transmission line*. One of the aims of the paper is to prove that for the subclass of response functions considered, the prescription based on P_T is, in some sense, optimal. Namely, we shall see that under quite general hypothesis, any local maximum of $|T(j\omega, D)|$ at a sufficiently large frequency ω_M will be arbitrary close to $P_T(\omega_M)$ and there will be an infinite sequence $\omega_n \to \infty$ such that $|T(j\omega_n, D)| = P_T(\omega_n)$. Observe that these statements hold for any $D > 0$, so that no single function $T(j\omega, D)$ for a particular D can attenuate "better" than $P_T(\omega)$, asymptotically. This means that if $P_T(\omega)$ does not meet the application specifications, chances are that the circuit described by $T(j\omega, D)$ would also not meet them. We say "chances are" because the peak control function controls the height of the peaks of $|T(j\omega, D)|$ but not their location in frequency; the peak frequencies are determined by the parameter D and hence by the particular line inserted in the system and as such, they may or may not be of importance for the system. We have illustrated the concept with the example in Section VI for which the peak control function indicates that the system may fail to attenuate the higher harmonics in the excitation voltage properly and we have chosen the transmission line in such a way that failure indeed happens. Truly, one may think that the example is a bit exaggerated as it relies on an amplifier with zero output resistance, but we did so in order to make the effect clearly visible; the presence of an output resistance would only diminish it but the concept would still apply.

The attenuation of transmission lines in this paper may be considered as negligible, given the line lengths usual for an RFID system. For instance, the above-mentioned example of

Section VI shows that a line delay of 6.32 ns may cause significant effects. For a RG-174 cable commonly employed in RFID and according to the producer's description **Error! Reference source not found.**, the mentioned delay would be achieved by 1.26 m of cable, for which the attenuation would be less than 0.15 dB at the standard RFID frequency of 13.56 MHz. Therefore all transmission lines will be assumed lossless.

The organization of the paper is as follows. Section II is devoted to basic definitions and theory. We introduce the peak control function associated to a response function, we define the concept of a simply controlled response function and prove the mathematical results that support the assertions concerning the utility of control functions in the optimization of a design. In Section III we establish the formula for a current ratio to be used in connection with class D amplifiers that comprise a transmission line. In Sections IV and V we study some response functions arising in the design of class D voltage mode and current mode amplifiers. It turns out that those functions are simply controlled which allows us to compute their peak control functions and apply the theory of Section II. In Section VI we discuss the optimization of an example voltage mode class amplifier based on criteria derived from the peak control function. The results of optimizations based on such criteria depend in general on the selected frequency domain and it would be the designer's task to make the best adequate choice for the application in view. In this context it is interesting to study the asymptotic behavior for large frequencies of the optimal value of a circuit component; a rigorous result of this kind for one of the components of the example circuit studied in Section VI is stated and proved in Section VII.

An abbreviated version [18] of our work that included the main results but none of the proofs was presented at the SIITME conference. In the present paper we have included all detailed proofs in order to achieve a presentation as much as possible self-contained of the theory of control functions and their applications to circuit design. We should emphasize that, although the theory exposed here follows the lines of the overview in [18], the presentation is technically different as it is centered around the concept of biexponential function which is new with respect to the named paper.

II. Definition and Properties of Control Functions

Consider the frequency response $T(j\omega, D)$ of a circuit comprising one lossless transmission line with delay D. The *peak control function* $P_T(\omega)$ for $T(j\omega, D)$ was defined in the Introduction as

$$P_T(\omega) = \sup_{D>0}\left|T(j\omega, D)\right|. \tag{2}$$

The computation of $P_T(\omega)$ is in general a difficult task. However there is a special class of frequency response functions for which the peak control function can be computed explicitly by means of elementary formulas. To this purpose we introduce first the concept of a *biexponential function* defined as a function $F(\omega, D)$ that admits the representation

$$F(\omega, D) = A(\omega)\exp(ja\omega D) + B(\omega)\exp(jb\omega D). \tag{3}$$

in which a, b are real numbers, $a \neq b$ and neither $A(\omega)$ nor $B(\omega)$ depend on D. In this definition D is no longer restricted to be positive but can be any real number.

The *lower control function* $L_F(\omega)$ and the *upper control function* $U_F(\omega)$ for the biexponential function $F(\omega, D)$ are defined by

$$L_F(\omega) = \inf_{D>0}\left|F(\omega, D)\right|, \quad U_F(\omega) = \sup_{D>0}\left|F(\omega, D)\right|. \tag{4}$$

A biexponential function has the advantage that the control functions L_F and U_F can be computed explicitly as shown by the following proposition.

PROPOSITION 1. *For any biexponential function* $F(\omega, D)$ *we have*

$$\begin{aligned} L_F(\omega) &= \inf_{D\in R}\left|F(\omega, D)\right| = \left|\left|A(\omega)\right| - \left|B(\omega)\right|\right|, \\ U_F(\omega) &= \sup_{D\in R}\left|F(\omega, D)\right| = \left|A(\omega)\right| + \left|B(\omega)\right|. \end{aligned} \tag{5}$$

Proof. Follows from the identity

$$\left|F(\omega, D)\right| = \left|A(\omega) + B(\omega)\exp(j(b-a)\omega D)\right| \tag{6}$$

and from the well-known relations

$$\begin{aligned} \sup_{x>0}\left|u + v\exp(jx)\right| &= \sup_{x\in R}\left|u + v\exp(jx)\right| = \left|u\right| + \left|v\right|, \\ \inf_{x>0}\left|u + v\exp(jx)\right| &= \inf_{x\in R}\left|u + v\exp(jx)\right| = \left|\left|u\right| - \left|v\right|\right| \end{aligned} \tag{7}$$

which are true for all complex numbers u, v.

The connection with response functions arises through the following definition. We shall say that the frequency response function $T(j\omega, D)$ is *simply controlled* if $T(j\omega, D)$ or the inverse function $1/T(j\omega, D)$ is biexponential.

PROPOSITION 2.

Let $T(j\omega, D)$ *be biexponential as in* (3). *Then*

$$P_T(\omega) = U_T(\omega) = \left|A(\omega)\right| + \left|B(\omega)\right|. \tag{8}$$

Let $1/T(j\omega, D)$ *be biexponential as in* (3). *Then*

$$P_T(\omega) = \frac{1}{L_{1/T}(\omega)} = \frac{1}{\left|\left|A(\omega)\right| - \left|B(\omega)\right|\right|}. \tag{9}$$

By definition we have $L_F(\omega) \le |F(\omega, D)| \le U_F(\omega)$ for every ω. In the following we shall address the question how close do $L_F(\omega)$ and $U_F(\omega)$ approximate $|F(\omega, D)|$ when $F(\omega, D)$ is biexponential. We shall prove that, under suitable hypothesis, a local extremum of $|F(\omega, D)|$ at some frequency ω_0 is approximated by either $L_F(\omega_0)$ or $U_F(\omega_0)$ to arbitrary precision. A further result shows that, again under quite general hypothesis, there is an infinity of points ω and ω' at which $|F(\omega, D)| = L_F(\omega)$ and $|F(\omega', D)| = U_F(\omega')$.

In the proofs we shall rely on the following formulas true for any complex function f of the real variable x, of which we have already made use in (1),

$$\begin{aligned} \frac{d}{dx}\left|f(x)\right| &= \frac{1}{\left|f(x)\right|}\mathrm{Re}\left(\overline{f(x)}\frac{d}{dx}f(x)\right), \\ \frac{d}{dx}\left|f(x)\right|^2 &= 2\,\mathrm{Re}\left(\overline{f(x)}\frac{d}{dx}f(x)\right). \end{aligned} \tag{10}$$

Below we shall make use of the function

$$\Omega(\omega, D) = \frac{dA(\omega)}{d\omega} + \frac{dB(\omega)}{d\omega}\exp(j(b-a)\omega D). \tag{11}$$

THEOREM 1. *Let* $F(\omega, D)$ *be biexponential as in* (3) *and let* ω_0 *be a stationary point of* $\left|F(\omega, D)\right|$, *that is, a point satisfying the relation* $\frac{d}{d\omega}\left|F(\omega_0, D)\right| = 0$ *(in particular, any local extremum of* $\left|F(\omega, D)\right|$*). Then*

$$L_F(\omega_0) \le \left|F(\omega_0, D)\right| \le \frac{L_F(\omega_0)}{\sqrt{1 - \dfrac{2\left|\Omega(\omega_0, D)\right|^2}{(b-a)^2 D^2 \left|A(\omega_0)B(\omega_0)\right|}}} \tag{12}$$

if $\operatorname{Re}\overline{A(\omega_0)}B(\omega_0)\exp(j(b-a)\omega_0 D) \le 0$,

$$\frac{U_F(\omega_0)}{\sqrt{1 + \dfrac{2\left|\Omega(\omega_0, D)\right|^2}{(b-a)^2 D^2 \left|A(\omega_0)B(\omega_0)\right|}}} \le \left|F(\omega_0, D)\right| \le U_F(\omega_0) \tag{13}$$

if $\operatorname{Re}\overline{A(\omega_0)}B(\omega_0)\exp(j(b-a)\omega_0 D) \ge 0$.

We shall of course assume that the quantities under the square roots are positive.

Proof. First we observe that the leftmost inequality in (12) and the rightmost inequality in (13) are consequences of the definition of the control functions.

We start by proving the following inequalities.

For all complex numbers u and v,

$$|u+v|^2 \le (|u| - |v|)^2 + 2\frac{(\operatorname{Im}\bar{u}v)^2}{|uv|} \text{ if } \operatorname{Re}\bar{u}v \le 0, \tag{14}$$

$$|u+v|^2 \ge (|u| + |v|)^2 - 2\frac{(\operatorname{Im}\bar{u}v)^2}{|uv|} \text{ if } \operatorname{Re}\bar{u}v \ge 0. \tag{15}$$

Indeed, we always have the inequalities

$$-1 \le \frac{\operatorname{Re}\bar{u}v}{|uv|} \le 1. \tag{16}$$

Assuming $-\operatorname{Re}\bar{u}v$ is positive, we may multiply by it both sides of the leftmost inequality in (16) and obtain

$$\operatorname{Re}\bar{u}v \le -\frac{(\operatorname{Re}\bar{u}v)^2}{|uv|}. \tag{17}$$

Observing that $|uv|^2 = (\operatorname{Re}\bar{u}v)^2 + (\operatorname{Im}\bar{u}v)^2$, we transform the above inequality as

$$\operatorname{Re}\bar{u}v \le -\frac{|uv|^2 - (\operatorname{Im}\bar{u}v)^2}{|uv|} = -|uv| + \frac{(\operatorname{Im}\bar{u}v)^2}{|uv|}. \tag{18}$$

It follows that

$$\begin{aligned} |u+v|^2 &= |u|^2 + |v|^2 + 2\operatorname{Re}\bar{u}v \\ &\le |u|^2 + |v|^2 - 2|uv| + 2\frac{(\operatorname{Im}\bar{u}v)^2}{|uv|} = \left||u| - |v|\right|^2 + 2\frac{(\operatorname{Im}\bar{u}v)^2}{|uv|}. \end{aligned} \tag{19}$$

When $\operatorname{Re}\bar{u}v \ge 0$, the second inequality is obtained in a similar way, by multiplying the rightmost inequality in (16) by $\operatorname{Re}\bar{u}v$.

Returning to the proof of the theorem, we first observe that because of the equality

$$\left|F(\omega, D/(b-a))\right| = \left|A(\omega) + B(\omega)\exp(j\omega D)\right| \tag{20}$$

it is enough to do the proof in the case $a = 0$, $b = 1$. We have for the derivative of F

$$\frac{dF(\omega, D)}{d\omega} = \Omega(\omega, D) + jDB\exp(j\omega D) \tag{21}$$

and for the derivative of $\left|F(\omega, D)\right|$

$$\begin{aligned} \frac{d}{d\omega}\left|F(\omega, D)\right| &= \frac{1}{\left|F(\omega, D)\right|}\operatorname{Re}\left(\overline{F}\frac{dF}{d\omega}\right) \\ &= \frac{\operatorname{Re}\left(\overline{F}\,\Omega(\omega, D)\right) - D\operatorname{Im}\left(\overline{A}B\exp(j\omega D)\right)}{\left|F(\omega, D)\right|}. \end{aligned} \tag{22}$$

Let us introduce the notations $g_0 = \exp(j\omega_0 D)$, $\Omega_0 = \Omega(\omega_0, D)$. Since ω_0 is a stationary point of $|F|$, we have from the above expression of the derivative

$$\operatorname{Im}\overline{A(\omega_0)}B(\omega_0)g_0 = \frac{1}{D}\operatorname{Re}\left(\overline{F(\omega_0, D)}\Omega_0\right) \tag{23}$$

from which it follows

$$\begin{aligned} \left(\operatorname{Im}\overline{A(\omega_0)}B(\omega_0)g_0\right)^2 &= \frac{1}{D^2}\left(\operatorname{Re}\overline{F(\omega_0, D)}\Omega_0\right)^2 \\ &\le \frac{1}{D^2}\left|F(\omega_0, D)\right|^2\left|\Omega_0\right|^2. \end{aligned} \tag{24}$$

Applying now (14) to $u = A(\omega_0)$ and $v = B(\omega_0)g_0$ under the hypothesis $\operatorname{Re}\overline{A(\omega_0)}B(\omega_0)g_0 \le 0$ and taking into account the (24), we obtain

$$\begin{aligned} \left|F(\omega_0, D)\right|^2 &\le \left(\left|A(\omega_0)\right| - \left|B(\omega_0)\right|\right)^2 + 2\frac{(\operatorname{Im}\overline{A(\omega_0)}B(\omega_0)g_0)^2}{\left|A(\omega_0)B(\omega_0)\right|} \\ &\le \left(\left|A(\omega_0)\right| - \left|B(\omega_0)\right|\right)^2 + 2\frac{\left|F(\omega_0, D)\right|^2\left|\Omega_0\right|^2}{D^2\left|A(\omega_0)B(\omega_0)\right|} \end{aligned} \tag{25}$$

from which (12) follows immediately. Similarly, the application of (15) under the hypothesis $\operatorname{Re}\overline{A(\omega_0)}B(\omega_0)g_0 \ge 0$ leads to (13).

In our applications in Sections IV – VI $A(\omega)$ and $B(\omega)$ will be rational functions of ω, that is, quotients of polynomials. Therefore one may speak about their degree in ω, defined as the difference between the degree of the numerator and the degree of the denominator. If m and n are the degree of A and B respectively, then assuming $\max(m, n) \ge 1$ and $|m - n| \le 1$, the quantity $|\Omega(\omega, D)|^2/|A(\omega)B(\omega)|$ becomes arbitrary small for large ω. Therefore, Theorem 1 shows that if $|F(\omega, D)|$ has a local extremum at a high enough frequency ω_0, then the extremum itself will be arbitrary close to either $L_F(\omega)$ or $U_F(\omega)$. However, if we know the nature of the extremum (that is, whether it is a minimum of a maximum), the theorem still does not tell us which of $L_F(\omega_0)$ or $U_F(\omega_0)$ will be close to $|F(\omega_0, D)|$. Of course we expect that the minimum would be approximated by $L_F(\omega_0)$ and the maximum by $U_F(\omega_0)$, but this has still to be proved. Such a proof is obtained below for the case $m = n$.

THEOREM 2. *Let* $F(\omega, D)$ *be biexponential as in* (3) *with* A *and* B *rational functions of equal degree* $m \ge 1$. *Then there is* ω_0 *such that* (12) *is satisfied at every local minimum* ω_m *of* $|F(\omega, D)|$ *in* (ω_0, ∞) *and* (13) *is satisfied at every local maximum* ω_M *of* $|F(\omega, D)|$ *in* (ω_0, ∞) *(*ω_0 *in the mentioned relations being replaced by* ω_m *and* ω_M *respectively).*

Proof. As before we may assume that $a = 0$ and $b = 1$. Consider the functions

$$\begin{aligned} &g(\omega, D) = \exp(j\omega D), \\ &\Phi(\omega, D) = 2\operatorname{Re}\left(\overline{F(\omega, D)}\Omega(\omega, D)\right), \\ &\Gamma(\omega, D) = 2\operatorname{Re}\left(\Omega\frac{d\overline{F}}{d\omega}\right) + 2\operatorname{Re}\left(\overline{F}\frac{d\Omega}{d\omega}\right) \\ &\quad - 2D\operatorname{Im}\left(B\frac{d\overline{A}}{d\omega}g\right) - 2D\operatorname{Im}\left(\overline{A}\frac{dB}{d\omega}g\right). \end{aligned} \tag{26}$$

From the hypotheses on A and B it follows that each term in $|\Phi(\omega, D)/A(\omega)B(\omega)|$ and $|\Gamma(\omega, D)/A(\omega)B(\omega)|$ converges to 0 as $\omega \to \infty$. Hence there is ω_0 such that

$$\left|\frac{\Phi(\omega,D)}{A(\omega)B(\omega)}\right| < \sqrt{2}D, \quad \left|\frac{\Gamma(\omega,D)}{A(\omega)B(\omega)}\right| < \sqrt{2}D^2 \tag{27}$$

for $\omega \in (\omega_0, \infty)$. Let $\omega_M \in (\omega_0, \infty)$ be a local maximum of $|F(\omega, D)|$ and hence of $|F(\omega, D)|^2$, the proof for a local minimum being similar. Let us introduce the notations $A_M = A(\omega_M)$, $B_M = B(\omega_M)$, $g_M = g(\omega_M, D)$. At a local maximum the first derivative vanishes while the second derivative is negative, therefore by (10)

$$\begin{aligned} 0 &= \frac{d}{d\omega}\left|F(\omega_M, D)\right|^2 \\ &= \Phi(\omega_M, D) - 2D\,\mathrm{Im}\left(\overline{A}_M B_M g_M\right), \\ 0 &\geq \frac{d^2}{d\omega^2}\left|F(\omega_M, D)\right|^2 \\ &= \Gamma(\omega_M, D) - 2D\,\mathrm{Im}\left(\overline{A}_M B_M \frac{dg}{d\omega}(\omega_M)\right) \\ &= \Gamma(\omega_M, D) - 2D^2\,\mathrm{Re}\left(\overline{A}_M B_M g_M\right). \end{aligned} \tag{28}$$

Dividing by $|A_M B_M|$ we obtain

$$\begin{aligned} &\mathrm{Re}\left(\frac{\overline{A}_M B_M g_M}{\left|A_M B_M\right|}\right) \geq \frac{\Gamma(\omega_M, D)}{2D^2\left|A_M B_M\right|} \\ &\geq -\frac{\left|\Gamma(\omega_M, D)\right|}{2D^2\left|A_M B_M\right|} > -\frac{1}{\sqrt{2}}. \end{aligned} \tag{29}$$

If we had $\mathrm{Re}\,\overline{A_M} B_M g_M \leq 0$, the above inequality would imply

$$\left|\mathrm{Re}\left(\frac{\overline{A}_M B_M g_M}{\left|A_M B_M\right|}\right)\right| < \frac{1}{\sqrt{2}}. \tag{30}$$

Together with

$$\left|\mathrm{Im}\left(\frac{\overline{A}_M B_M g_M}{\left|A_M B_M\right|}\right)\right| = \frac{\left|\Phi(\omega_M, D)\right|}{2D\left|A_M B_M\right|} < \frac{1}{\sqrt{2}} \tag{31}$$

this would in turn imply

$$\begin{aligned} 1 &= \left|\mathrm{Re}\left(\frac{\overline{A}_M B_M g_M}{\left|A_M B_M\right|}\right)\right|^2 + \left|\mathrm{Im}\left(\frac{\overline{A}_M B_M g_M}{\left|A_M B_M\right|}\right)\right|^2 \\ &< \frac{1}{2} + \frac{1}{2} = 1 \end{aligned} \tag{32}$$

which is a contradiction. Consequently $\mathrm{Re}\,\overline{A_M} B_M g_M > 0$ and Theorem 1 shows that (13) is satisfied.

THEOREM 3. *Let* $F(\omega, D)$ *admit the representation* (3), *let* θ *be any complex number of unit modulus and let* $I = [\omega_1, \omega_2]$ *be a closed interval of length* $|2\pi/(b - a)D|$ *such* $\theta = \exp(j(b - a)\omega_1 D)$. *Assume that for every* ω *in* I *the following conditions are fulfilled*:

i) $A(\omega) \neq 0$ and $B(\omega) \neq 0$;

ii) $A(\omega)/|A(\omega)| \neq \theta B(\omega)/|B(\omega)|$.

Then there is ω_0 *in* (ω_1, ω_2) *such that* $|F(\omega_0, D)| = U_F(\omega_0)$.

A similar statement holds for $L_F(\omega)$.

Proof. As in the preceding proofs we may assume that $a = 0$ and $b = 1$. By replacing the function $B(\omega)$ with the function $\theta B(\omega)$ we may also assume that $\omega_1 = 0$. Let C_1 be the set of complex numbers of unit moduli from which we exclude the number 1. Consider the function $G(\omega)$ defined on $I = [0, 2\pi/D]$ by

$$G(\omega) = \frac{A(\omega)/B(\omega)}{\left|A(\omega)/B(\omega)\right|}. \tag{33}$$

Because of conditions i) and ii), G is a continuous function with values into C_1. The function $H(\omega)$ defined on $J = (0, 2\pi/D)$ by $H(\omega) = \exp(j\omega D)$ establishes a bijective map between J and C_1 whose inverse H^{-1} is continuous. Consequently, the function φ defined as the composition of H^{-1} and G maps continuously I into J and satisfies $\exp(j\varphi(\omega)D) = G(\omega)$ for every ω in I. The continuous function χ defined on I by $\chi(\omega) = \varphi(\omega) - \omega$ satisfies $\chi(0) > 0$ and $\chi(2\pi/D) < 0$; consequently there is ω_0 in J such that $\chi(\omega_0) = 0$ ([19], subsection 5.22, p. 140). For this ω_0 we have $\exp(j\omega_0 D) = \exp(j\varphi(\omega_0)D) = G(\omega_0)$ which implies

$$\begin{aligned} \left|F(\omega_0, D)\right| &= \left|A(\omega_0) + B(\omega_0)\frac{A(\omega_0)/B(\omega_0)}{\left|A(\omega_0)/B(\omega_0)\right|}\right| \\ &= \left|A(\omega_0)\right| + \left|B(\omega_0)\right| = U_F(\omega_0) \end{aligned} \tag{34}$$

and the proof is complete.

When A and B are rational functions the limit

$$l = \lim_{\omega\to\infty} \frac{A(\omega)/B(\omega)}{\left|A(\omega)/B(\omega)\right|} \tag{35}$$

always exist, hence we are certain that conditions i) and ii) of Theorem 3 are fulfilled for ω larger than some ω_0 provided that we choose $\theta \neq l$. Therefore, according to the theorem, in every subinterval (ω_1, ω_2) of (ω_0, ∞) whose length is $|2\pi/(b - a)D|$ and for which $\exp(j(b - a)\omega_1 D) = \theta$, there will be an ω for which $|F(\omega, D)| = U_F(\omega)$.

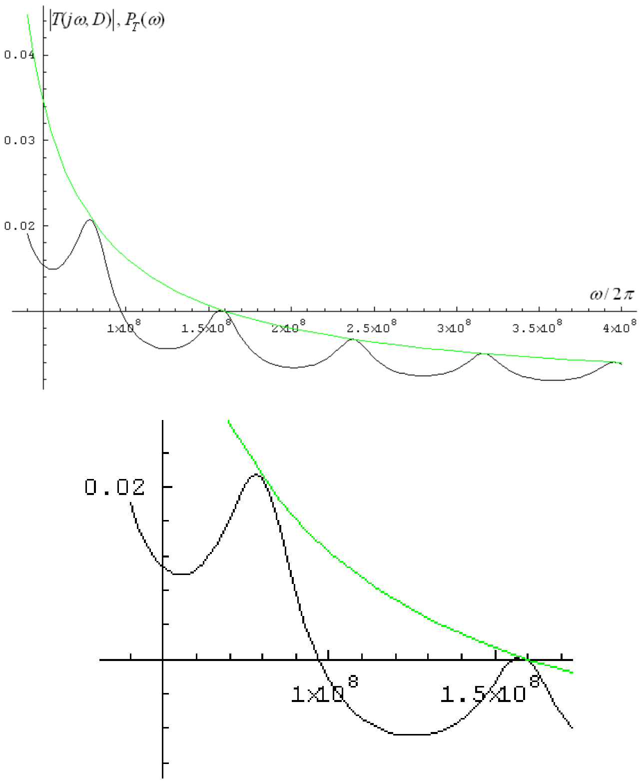

Figure 2. Upper graph: frequency response function together (lower trace) with its peak control function (upper trace). Lower graph: close-up of a detail of the upper graph.

In conclusion, let us summarize the findings of this section that are significant for the applications we have in view.

The utility of the peak control function $P_T(\omega)$ of a simply controlled response function $T(j\omega, D)$ stems from the following properties that are consequences of the above proved results.

i) $|T(j\omega, D)| \leq P_T(\omega)$ for any frequency ω. Therefore if $P_T(\omega)$ is well behaved for large frequencies, $T(j\omega, D)$ will also be so.

ii) Any local maximum of $|T(j\omega, D)|$ at a sufficiently large frequency ω_M will be arbitrary close to $P_T(\omega_M)$, under quite general hypothesis stated by Theorems 1 and 2.

iii) If A and B in the representation (3) of $T(j\omega, D)$ or of $1/T(j\omega, D)$ are rational functions, there is a frequency ω_0 such that (ω_0, ∞) can be partitioned into subintervals of equal length $|2\pi/(b-a)D|$, each of them containing an ω for which $|T(j\omega, D)| = P_T(\omega)$.

The relation between the response function and its peak control function is better understood with the aid of a graphical example. In the upper graph of Fig. 2 one sees the oscillating $|T(j\omega, D)|$ lying below the monotone decreasing $P_T(\omega)$ (property i) and one remarks the presence of a sequence of frequencies ω_n at which $|T(j\omega_n, D)| = P_T(\omega_n)$ (property iii). The lower graph shows a close-up of a local maximum at ω_M of $|T(j\omega, D)|$. One remarks that $P_T(\omega_M)$ does not coincide with $|T(j\omega_M, D)|$ but is close to it and the approximation becomes better as frequency increases (property ii).

In order not to complicate the notations excessively, in the next sections we shall not write the dependence on ω of the various functions explicitly when this dependence will be clear from the context.

III. The Current Ratio for a Lossless Transmission Line

We shall need the ratio of the currents at the ends of a lossless transmission line of length l and delay D connected at a source providing the harmonic excitation at one end and terminated in a load impedance Z_L at the other.

As well known [20], the voltage and current along the line are represented as

$$\begin{aligned} V(x) &= V_+ \exp(-j\omega x / v) + V_- \exp(j\omega x / v), \\ I(x) &= I_+ \exp(-j\omega x / v) - I_- \exp(j\omega x / v) \end{aligned} \tag{36}$$

where V_+ and V_- are constants determined by the boundary conditions, v is the propagation speed along the line, $I_+ = V_+/Z_0$, $I_- = V_-/Z_0$ and Z_0 is the characteristic line impedance.

At the source end ($x = 0$) we have

$$I_S = I_+ - I_-, \quad I_- = \Gamma_S I_+ \tag{37}$$

where Γ_S is the reflection coefficient at the source end. Solving for I_+ and I_- we obtain at the load end ($x = l$)

$$\begin{aligned} I_L &= I_+ \exp(-j\omega l / v) - I_- \exp(j\omega l / v) \\ &= I_S \frac{\exp(-j\omega D) - \Gamma_S \exp(j\omega D)}{1 - \Gamma_S}. \end{aligned} \tag{38}$$

The reflection coefficient Γ_L at the load end is given by $\Gamma_L = (Z_L - Z_0)/(Z_L + Z_0)$ and is related to Γ_S by $\Gamma_S / \Gamma_L = \exp(-2j\omega D)$. Substituting these relations in (38) we obtain the ratio we look for as

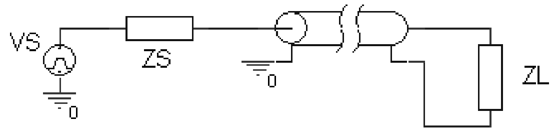

Figure 3. Model of voltage-mode class D amplifier.

$$\frac{I_L}{I_S} = \frac{Z_0}{(Z_0 + jZ_L \tan(\omega D))\cos(\omega D)}. \tag{39}$$

IV. The Upper Control Function for a Voltage-Mode Class D Amplifier

Consider the voltage-mode class D amplifier redrawn in a more condensed form in Fig. 3, by lumping the power source, the MOSFET switches and the transformer into the voltage source V_S. For ease of notation we shall use impedances and admittances normalized to Z_0 and denoted with lower case. The impedance of the load connected to the transmission line equals $z_L = r_L + jx_L$. At the source end is connected an impedance $z_S = r_S + jx_S$ that includes the source impedance as well as any additional filter in series with the line.

As explained in the Introduction, the source V_S drives the circuit with a voltage square wave. Since we need to know the harmonic content of the current through the load, the frequency response of the circuit must be analyzed not only at the nominal frequency but also at the higher harmonics. To this purpose we replace V_S by a harmonic voltage excitation $V\exp(j\omega t)$ and we determine the frequency response $T(j\omega, D) = Z_0 I_L(j\omega, D)/V$ where $I_L(j\omega, D)$ is the load current (we multiplied by Z_0 for having a dimensionless function). The current $I_S(j\omega, D)$ entering the line at the source end equals $V/Z_0(z_S + z)$, where z is the impedance looking into the line at the source end. As well known [20], the latter is given by

$$z = \frac{z_L + j\tan(\omega D)}{1 + jz_L \tan(\omega D)}. \tag{40}$$

The current I_L that exits the line at the load is given by (39). Therefore the response we are interested in is

$$\begin{aligned} T(j\omega, D) &= \frac{Z_0 I_L(\omega, D)}{V} \\ &= \frac{1}{z_S + \dfrac{z_L + j\tan(\omega D)}{1 + jz_L \tan(\omega D)}} \frac{1}{(1 + jz_L \tan(\omega D))\cos(\omega D)} \\ &= \frac{1}{z_S(1 + jz_L \tan(\omega D)) + z_L + j\tan(\omega D)} \frac{1}{\cos(\omega D)}. \end{aligned} \tag{41}$$

In order to compute the peak control function $P_T(\omega)$ we shall show that $1/T(j\omega, D)$ is biexponential. After replacing in (41) $\tan(\omega D)$ with $\sin(\omega D)/\cos(\omega D)$ and using the relations

$$\begin{aligned} \cos(\omega D) &= \frac{\exp(j\omega D) + \exp(-j\omega D)}{2}, \\ \sin(\omega D) &= \frac{\exp(j\omega D) - \exp(-j\omega D)}{2j}, \end{aligned} \tag{42}$$

we find after regrouping the exponentials

$$\frac{1}{T(j\omega, D)} = A(\omega)\exp(j\omega D) + B(\omega)\exp(-j\omega D) \tag{43}$$

with

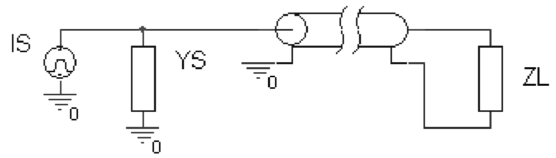

Figure 4. Model of current-mode class D amplifier.

$$\begin{aligned} A(\omega) &= \frac{1}{2}(1+z_S(j\omega))(1+z_L(j\omega)), \\ B(\omega) &= -\frac{1}{2}(1-z_S(j\omega))(1-z_L(j\omega)). \end{aligned} \tag{44}$$

The peak control function $P_T(\omega)$ is then computed by Proposition 2 ii),

$$P_T = \frac{1}{\left\| A \right| - \left| B \right\|} = \frac{2}{\left\| 1+z_S \right| \left| 1+z_L \right| - \left| 1-z_S \right| \left| 1-z_L \right\|}. \tag{45}$$

Because $|A|$ and $|B|$ are large for large frequencies, it will be convenient to re-express P_T in a form that does not contain differences of large quantities. For this purpose we write

$$\frac{1}{|A|-|B|} = \frac{|A|+|B|}{|A|^2-|B|^2} \tag{46}$$

and we compute the denominator as

$$\begin{aligned} |A|^2-|B|^2 &= \left(1+2r_S+|z_S|^2\right)\left(1+2r_L+|z_L|^2\right)/4 - \\ &\left(1-2r_S+|z_S|^2\right)\left(1-2r_L+|z_L|^2\right)/4 \\ &= (r_S+r_L)(1+r_Sr_L)+x_S^2r_L+x_L^2r_S. \end{aligned} \tag{47}$$

The final result is

$$P_T = \frac{1}{2}\frac{\sqrt{((1+r_S)^2+x_S^2)((1+r_L)^2+x_L^2)}+\sqrt{((1-r_S)^2+x_S^2)((1-r_L)^2+x_L^2)}}{(r_S+r_L)(1+r_Sr_L)+x_S^2r_L+x_L^2r_S}. \tag{48}$$

Assuming that x_S and x_L are large for large frequencies while r_S and r_L stay bounded, we find the asymptotic form of P_T as

$$P_T = \frac{|x_Sx_L|}{x_S^2r_L+x_L^2r_S}. \tag{49}$$

The expression for P_T gets a simpler form in case r_S or r_L vanish. Assuming $r_S = 0$, P_T reduces to

$$\frac{\sqrt{(1+r_L)^2+x_L^2}+\sqrt{(1-r_L)^2+x_L^2}}{2r_L\sqrt{1+x_S^2}}. \tag{50}$$

V. The Peak Control Function for a Current-Mode Class D Amplifier

Consider the current-mode class D amplifier shown in Fig. 4. The discussion in this section parallels that of Section IV, with the difference that instead of V_S we have now a current source I_S that drives the circuit with a current square wave. The impedance of the load connected to the transmission line equals $z_L = r_L + jx_L$. At the source end is connected an admittance $y_S = g_S + jb_S$ that includes the source admittance as well as any additional filter in parallel with the line.

For analyzing the harmonic content of the current through the load, we replace I_S by a harmonic current excitation $I\exp(j\omega)$ and we determine the frequency response $T(j\omega, D) = I_L(j\omega, D)/I$ where $I_L(j\omega, D)$ is the load current. The current entering the line at the source end equals $I\,y/(y_S + y)$, where y is the admittance looking into the line at the source end given by

$$y = \frac{1+jz_L\tan(\omega D)}{z_L+j\tan(\omega D)}. \tag{51}$$

The current $I_L(j\omega, D)$ that exits the line at the load is given by (39) and the frequency response is

$$\begin{aligned} T(j\omega, D) &= \frac{I_L}{I} \\ &= \frac{\dfrac{1+jz_L\tan(\omega D)}{z_L+j\tan(\omega D)}}{y_S+\dfrac{1+jz_L\tan(\omega D)}{z_L+j\tan(\omega D)}}\frac{1}{(1+jz_L\tan(\omega D))\cos(\omega D)} \\ &= \frac{1}{1+jz_L\tan(\omega D)+y_S(z_L+j\tan(\omega D))}\frac{1}{\cos(\omega D)}. \end{aligned} \tag{52}$$

Proceeding as in the previous section we find

$$A = \frac{1}{2}(1+y_S)(1+z_L), \quad B = \frac{1}{2}(1-y_S)(1-z_L). \tag{53}$$

The peak control function is therefore

$$P_T = \frac{1}{\left\| A \right| - \left| B \right\|} = \frac{2}{\left\| 1+y_S \right| \left| 1+z_L \right| - \left| 1-y_S \right| \left| 1-z_L \right\|}. \tag{54}$$

As previously we re-express P_T in a form that does not contain differences of large quantities:

$$P_T = \frac{1}{2}\frac{\sqrt{((1+g_S)^2+b_S^2)((1+r_L)^2+x_L^2)}+\sqrt{((1-g_S)^2+b_S^2)((1-r_L)^2+x_L^2)}}{(g_S+r_L)(1+g_Sr_L)+b_S^2r_L+x_L^2g_S}. \tag{55}$$

Assuming that y_S and x_L are large for large frequencies while g_S and r_L stay bounded, we find the asymptotic form of P_T as

$$P_T = \frac{|b_Sx_L|}{b_S^2r_L+x_L^2g_S}. \tag{56}$$

The expression for P_T gets a simpler form in case g_S or r_L vanish. Assuming $g_S = 0$, P_T reduces to

$$\frac{\sqrt{(1+r_L)^2+x_L^2}+\sqrt{(1-r_L)^2+x_L^2}}{2r_L\sqrt{1+b_S^2}}. \tag{57}$$

VI. Analysis of an Example Circuit

Consider the voltage-mode amplifier of Fig. 5A. If we assume that V_S delivers a square wave voltage as is the case with class D amplifiers, then the current flowing into the antenna coil will be nearly sinusoidal due to the intrinsic filtering properties of the antenna resonant circuit. In order to assess how effective is the antenna circuit in reducing the unwanted harmonics we compare the amplitude I_{L0} of the nominal current flowing into the antenna when powered by a source $V\exp(j\omega_0 t)$ at the resonant frequency ω_0 of the antenna circuit with the amplitude $|I_L(j\omega)|$ of the current that flows when we use a source $V\exp(\omega t)$ of the same amplitude V but at some arbitrary frequency ω. We are therefore interested in the response function $T(j\omega) = I_L(j\omega)/I_{L0} = R_AI_L(j\omega)/V$ that describes the attenuation of the upper harmonics with respect to the nominal current; we have used the relation $I_{L0} = V/R_A$ which is true because the antenna circuit is tuned to ω_0. The Spice AC analysis has been used for representing $T(j\omega)$ in left side of Fig. 6. The analysis has

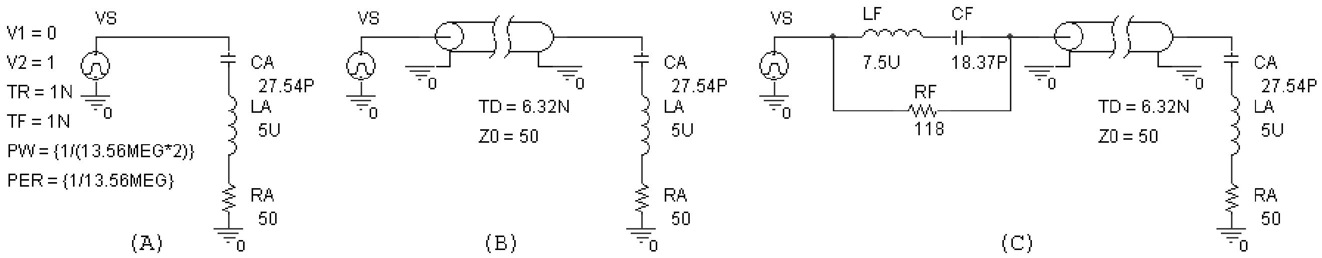

Figure 5. Spice simulation of voltage-mode class D amplifier without transmission line (A), with transmission line (B) and with filter at the source end of transmission line (C).

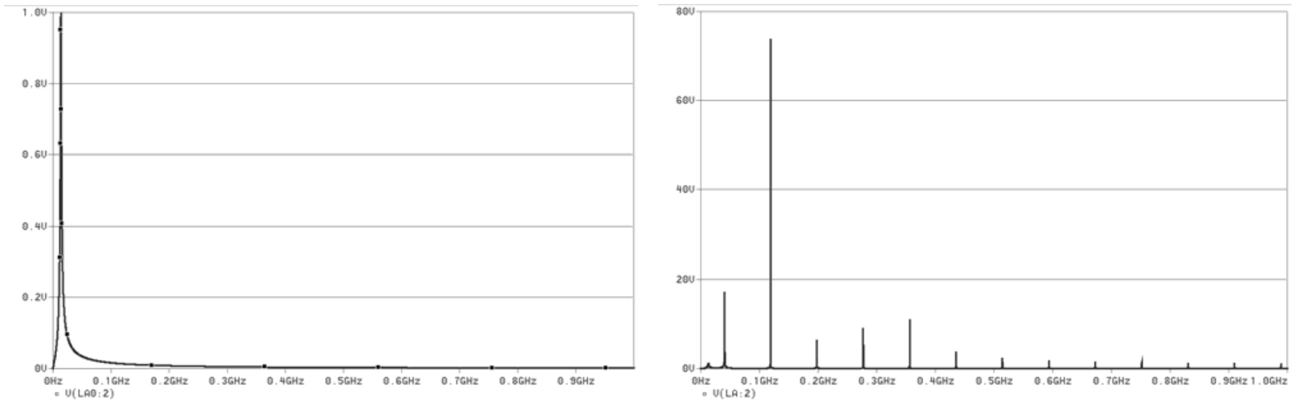

Figure 6. Results of Spice AC analysis of schematics of fig. 5A (left) and of fig. 5B (right).

swept the frequency over the interval 10 MHz – 1 GHz and computed the frequency response at 10000 points. One may see the rapid decrease of the antenna current outside resonance, which confirms the intrinsic filtering property of the circuit.

We turn now our attention to the case represented in Fig. 5B, where a transmission line of characteristic impedance Z_0 = 50 Ohm has been inserted between V_S and the antenna circuit. We are again interested in comparing $I_L(j\omega, D)$ with the nominal current I_{L0}. We observe that the amplitude of the latter is still given by V/R_A, as at resonance the circuit impedance reduces to R_A since the latter is matched to the line impedance. Therefore the frequency response of interest is $T(j\omega, D) = R_A I_L(j\omega, D)/V_S$. When we represent the latter by using an AC analysis under the same Spice settings as above, we obtain the result of right side of Fig. 6. We see that the presence of the transmission line has added a new effect in the form of a series of resonant peaks. Since the figure seems to suggest that the peak heights approach zero as frequency increases, one may be inclined to think, by analogy with left side of Fig. 6, that the filtering property and the removal of current harmonics are working in this case also. However, this turns to be completely false: not only the peak heights do not approach zero, but also they tend to infinity as the frequency increases. We may convince ourselves that this is the case with the aid of the theory of the peak control function; the fact that in our figure the peak heights approach zero is an artifact due to the finite resolution of the Spice AC analysis

According to (50) and taking into account that in our case r_L = 1 and z_S = 0, the peak control function $P_T(\omega)$ for the frequency response $T(j\omega, D)$ is given by

$$P_T(\omega) = \sqrt{1 + x_L(\omega)^2/4} + \left|x_L(\omega)\right|/2 \quad (58)$$

where $x_L(\omega) = \left(L_A\omega - 1/C_A\omega\right)/Z_0$. From the above relation and the general theory of Section II we may then infer that the heights of the peaks of $|T(j\omega, D)|$ do indeed tend to infinity.

In order to check that the behavior of $|T(j\omega, D)|$ is indeed predicted by $P_T(\omega)$ in the sense explained in Section II, we recalculate the peaks via separate AC analyses around each of them, increasing the resolution as the frequency increases. The results are shown in Table 1; the resolution has been increased by narrowing the interval (second column of table) around each peak on which the analysis has been performed while keeping the same number of points, 10000. One remarks the very good agreement between the peak heights and the values of $P_T(\omega)$ at the peak frequencies.

TABLE 1. COMPARISON BETWEEN SPICE AC ANALYSIS AND PEAK CONTROL FUNCTION.

Frequency (MHz)	Analysis Interval (MHz)	$\lvert T(j\omega, D)\rvert$ from Spice	$P_T(\omega)$
40.663	40.4-40.9	22.751	22.7509
119.012	118.8-119.2	73.819	73.8198
197.988	197.9-198.1	123.823	123.824
277.044	277-277.08	173.659	173.66
356.125	356.08-356.16	223.438	223.44
435.219	435.2-435.24	273.193	273.194
514.319	514.3-514.34	322.93	322.935
593.423	593.4-593.44	372.655	372.667
672.528	672.51-672.55	422.392	422.392
751.636	751.625-751.645	472.112	472.115
830.745	830.735-830.755	521.83	521.835
909.854	909.85-909.858	571.553	571.553

As pointed out in the Introduction, high peaks in $T(j\omega, D)$ may result in high harmonic content of the antenna current, in case the frequencies of some harmonics in the square wave voltage produced by V_S happen to be near the peak frequencies. In Fig. 5B we have chosen on purpose the line delay so that the third harmonic of the nominal frequency of 13.56 MHz lies very close to the peak at 40.663 MHz in the first line of Table 1. Simulation shows (lower half of Fig. 7) the presence of an over-amplified third harmonic in the waveform of the antenna current. This is to be contrasted with upper half of Fig. 7 that shows the antenna current with the transmission line removed.

According to (44), the term B vanish identically if $z_S = 1$, that is, if the source impedance is resistive and matched to the line impedance. A vanishing B would mean, according to (**3**), that the transmission line is practically absent from the frequency response and its presence in the circuit will not introduce any unwanted effects. However, a source impedance of resistive type matched to the line impedance would dissipate a significant amount of power and this would defy the purpose of a class D amplifier as a high efficiency power source. The power dissipation issue may be alleviated if in parallel with R_F we add a series LC filter tuned to ω_0 as in Fig. 5C that would provide a zero-impedance path for the main harmonic of the current. In such a situation we have

$$r_S(\omega) = R_F X_F^2(\omega) / Z_0(R_F^2 + X_F^2(\omega)) \ ,$$

$$x_S(\omega) = X_F(\omega) R_F^2 / Z_0(R_F^2 + X_F^2(\omega)) \, , \tag{59}$$

where $X_F(\omega) = L_F\omega - 1/C_F\omega$ is the reactance of the LC filter. As $x_S(\omega) \to 0$ and $r_S(\omega) \to R_F/Z_0$, the presence of the term $x_L(\omega)^2 r_S(\omega)$ in the denominator of (48) ensures that $P_T(\omega) \to 0$ as $\omega \to \infty$ and so is well behaved. Simulation of the modified circuit of Fig. 5C shows that the antenna current has resumed its sinusoidal form.

Fig. 8 shows the frequency dependence of P_T for the component values of Fig. 5C and several values of $r_F = R_F/Z_0$. One remarks that for high enough frequencies ω, the curve that gives the smallest value for $P_T(\omega)$ does not correspond to $r_F = 1$ but to $r_F = 2.36$. In fact we shall prove in the next section that the value of r_F which gives the smallest value of $P_T(\omega)$ for high enough frequencies satisfies the equation

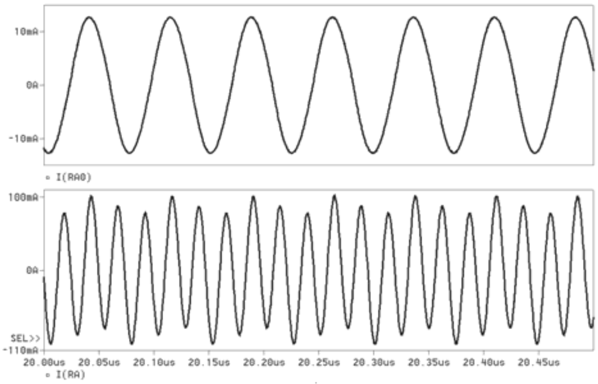

Figure 7. Results of Spice analysis showing the load current in schematic of Fig. 5A (upper) and of Fig. 5B (lower).

$$r_F^3(r_F^2 - 2) - (r_F^2 - 1)^2 (L_F / L_A)^2 = 0 \, . \tag{60}$$

The curve in Fig. 8 labeled $r_F = \infty$ corresponds to the case when R_F has been removed from the filter. The pure reactive filter will still be able to compensate for the effects of the transmission line, the difference being that in this case $P_T(\omega)$ does no longer converge to 0 as $\omega \to \infty$ but to the finite value $Z_0 L_A / R_A L_F$ according to (49).

In the case of a current-mode amplifier, the peak control function may help in deciding whether the parallel LC filter has to be inserted at the source end or at the load end of the transmission line. A discussion based on (55) along the same lines as above shows that having the filter at the load end and $y_S = 0$ results in a P_T growing to infinity while having the filter at the source end results in a P_T converging to a finite non-zero limit. The limit will be zero if a resistor is added in series with the filter.

VII. An Asymptotic Result

Refer to the circuit of Fig. 5C for which the peak control function P_T was shown to be given by (45) where

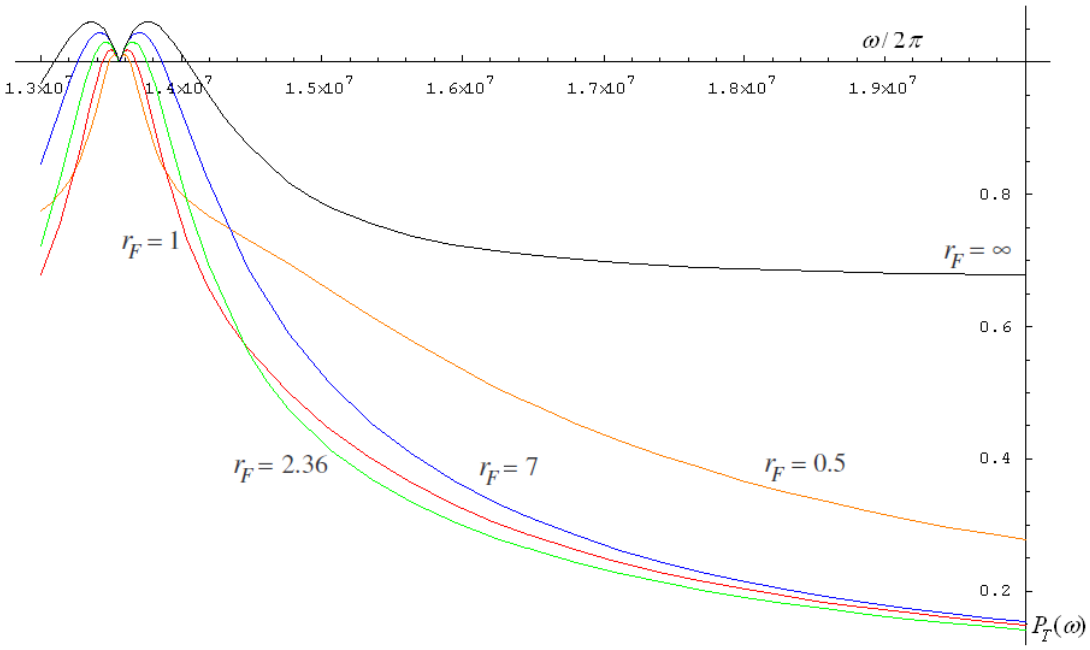

Figure 8. Frequency dependence of peak control function.

$$z_S = \frac{jr_F x_F}{r_F + jx_F}, \quad r_F = \frac{R_F}{Z_0}, \quad x_F(\omega) = \frac{L_F\omega - \frac{1}{C_F\omega}}{Z_0},$$
$$z_L = 1 + jx_A, \quad x_A(\omega) = \frac{L_A\omega - \frac{1}{C_A\omega}}{Z_0}. \tag{61}$$

In Section VI it was pointed out that for the given circuit, the "standard" choice of a source resistor matched to the line ($r_F = 1$) does not represent the optimal choice from the point of view of minimizing the peak control function (45). Our purpose in the following is to prove the result stated in Section VI concerning the asymptotic behavior of the value of r_F that minimizes (45).

THEOREM 4. *Assume that L_A, C_A, L_F and C_F are fixed. For every frequency ω let r_ω be the value of r_F that minimizes* (45) *with z_S and z_L computed at that frequency. Then as $\omega \to \infty$, r_ω converges to the unique positive solution r of the equation*

$$r^3(r^2 - 2) - (r^2 - 1)^2 (L_F / L_A)^2 = 0. \tag{62}$$

The proof will be divided into several stages.

We start by observing that minimizing P_T is equivalent to maximizing the function

$$L = \left\| 1 + z_S \right| \left| 1 + z_L \right| - \left| 1 - z_S \right| \left| 1 - z_L \right\|. \tag{63}$$

Since Re $z_S \geq 0$ and Re $z_L \geq 0$ we have $|1 + z_S| \geq |1 - z_S|$ and $|1 + z_L| \geq |1 - z_L|$, implying that we can drop the modulus in the expression of L,

$$L = \left| 1 + z_S \right| \left| 1 + z_L \right| - \left| 1 - z_S \right| \left| 1 - z_L \right|. \tag{64}$$

We shall find more convenient to change from the variable r_F to the variable $g = 1/r_F$ and perform the maximization with respect to this latter variable. We introduce the admittance $y = 1/z_S$ and write its dependence on g as $y = g + jb$, where

$$b(\omega) = -\frac{Z_0}{L_F\omega - \frac{1}{C_F\omega}}. \tag{65}$$

In the following we shall assume implicitly the dependencies on ω and write them explicitly only when necessary.

We shall maximize L by equating to 0 its derivative with respect to g, so we need expressions for the required derivatives.

LEMMA 1.

$$\frac{d}{dg}\left|1 + z_S\right| = -\frac{\operatorname{Re} y(1+y)}{|y|^3 |1+y|} = -\frac{g + g^2 - b^2}{|y|^3 |1+y|},$$
$$\frac{d}{dg}\left|1 - z_S\right| = -\frac{\operatorname{Re} y(1-y)}{|y|^3 |1-y|} = -\frac{g - g^2 + b^2}{|y|^3 |1-y|}. \tag{66}$$

The proof follows from (10).

LEMMA 2. For every complex number $y = g + jb$ we have

$$|1 - y|^2 \left(\operatorname{Re} y(1+y)\right)^2 - |1 + y|^2 \left(\operatorname{Re} y(1-y)\right)^2 = 4b^2 g(2g^2 - 2b^2 - 1). \tag{67}$$

The proof follows by direct computation.

LEMMA 3. $|1 + z_S| - |1 - z_S|$ is strictly increasing as a function of g on $[0, \sqrt{b^2 + 1/2})$ and strictly decreasing on $(\sqrt{b^2 + 1/2}, \infty]$.

Proof. By Lemma 1, the derivative of the function under consideration at $g = 0$ equals

$$\frac{2b^2}{|b|^3 |1 + jb|}, \tag{68}$$

therefore it is strictly positive. Suppose that the derivative vanishes at g_0. Then at such point we have

$$\left(\frac{d}{dg}\left|1 + z_S\right|\right)^2 = \left(\frac{d}{dg}\left|1 - z_S\right|\right)^2 \tag{69}$$

and an application of Lemmas 1 and 2 yields $4b^2 g_0(2g_0^2 - 2b^2 - 1) = 0$. Since $b \neq 0$ and $g_0 \neq 0$, the latter equality implies $g_0^2 = b^2 + 1/2$. Hence the derivative does not vanish on $[0, \sqrt{b^2 + 1/2})$ and consequently must be strictly positive there, implying that the function is strictly increasing. Likewise, the derivative does not vanish on $(\sqrt{b^2 + 1/2}, \infty]$; to find its sign on that interval, observe that for g large enough we have $g + g^2 - b^2 > 0$ and $g - g^2 + b^2 < 0$ which by Lemma 1 implies that the sign is negative.

LEMMA 4. $|1 + z_S|$ is strictly increasing as a function of g on $[0, \min(1, b^2/2))$ and strictly decreasing on $(|b|, \infty)$.

Proof. The derivative of the function under consideration is given by (66). If g belongs to the first interval, then $g + g^2 \leq 2g < b^2$ implying that the function is strictly increasing. If on the other hand g belongs to the second interval, then $g + g^2 > g^2 > b^2$ implying that the function is strictly decreasing.

LEMMA 5. For every $K > 0$, the equation

$$(1 - g^2)^2 g + K(2g^2 - 1) = 0 \tag{70}$$

has a unique positive solution.

Proof. Consider the function

$$f(g) = \frac{(1 - g^2)^2 g}{1 - 2g^2}. \tag{71}$$

Its derivative is given by

$$\frac{d}{dg} f(g) = \frac{(g^2 - 1)(-6g^4 + 3g^2 - 1)}{(1 - 2g^2)^2}. \tag{72}$$

The first factor in the numerator is negative on $[0, \sqrt{1/2})$ while the second factor has complex roots and is negative everywhere. Therefore f increases to ∞ on $[0, \sqrt{1/2})$ which shows the existence and uniqueness of the root of (70) on that interval. If now g_0 is any positive root of (70), then $(2g_0^2 - 1) = -(1 - g_0^2)^2 g_0 / K < 0$ which shows that g_0 must belong to $[0, \sqrt{1/2})$ and the uniqueness of the positive root is proved.

Proof of Theorem 4. Maximizing L is equivalent to maximizing $L/|x_A|$ which we write in the form

$$\left|1+z_S\right|\sqrt{1+4b_A^2}-\left|1-z_S\right|, \quad b_A(\omega)=-\frac{1}{x_A(\omega)}. \tag{73}$$

Writing the above expression as

$$\left|1+z_S\right|\left(\sqrt{1+4b_A^2}-1\right)+\left|1+z_S\right|-\left|1-z_S\right| \tag{74}$$

shows that $L/|x_A|$ as a function of g is increasing on $[0, \min(\sqrt{1/2}, b^2/2))$ and decreasing on $(\sqrt{b^2+1/2}, \infty]$ as being a sum of functions with monotony properties on the respective intervals by Lemmas 3 and 4. Consequently there is g_ω that maximizes $L/|x_A|$ and satisfies the inequalities

$$\min(\sqrt{1/2}, b^2/2) \le g_\omega \le \sqrt{b^2+1/2}. \tag{75}$$

As $b \to 0$ when $\omega \to \infty$, in the following we shall restrict ω to an interval $[\omega_0, \infty)$ so that $b^2 < 1/2$. With this assumption it follows that g_ω satisfies

$$b^2/2 \le g_\omega \le 1. \tag{76}$$

In particular the above inequalities show that g_ω is bounded. Therefore all we have to prove is that all limit points of g_ω coincide and satisfy (70) with $K=(L_A/L_F)^2$; recall that in analysis one defines a limit point as a point g_0 with the property that every interval $[\alpha, \infty)$ contains a point ω such that g_ω is arbitrary close to g_0 ([19], subsection 4.64, pp. 124–125). By the uniqueness assertion of Lemma 5, it suffices to prove that any such limit point satisfies (70).

Since the derivative of $L/|x_A|$ with respect to g vanishes at g_ω, we have by taking squares

$$\left(1+4b_A^2\right)\left(\frac{d}{dg}\left|1+z_S\right|\right)^2=\left(\frac{d}{dg}\left|1-z_S\right|\right)^2 \tag{77}$$

which by Lemma 1 implies

$$\left(1+4b_A^2\right)\left|1-y\right|^2\left(\operatorname{Re} y(1+y)\right)^2=\left|1+y\right|^2\left(\operatorname{Re} y(1-y)\right)^2. \tag{78}$$

This may be rewritten as

$$\begin{aligned}&4b_A^2\left|1-y\right|^2\left(\operatorname{Re} y(1+y)\right)^2\\&=\left|1+y\right|^2\left(\operatorname{Re} y(1-y)\right)^2-\left|1-y\right|^2\left(\operatorname{Re} y(1+y)\right)^2\end{aligned} \tag{79}$$

which by Lemma 2 gives

$$b_A^2\left((1-g_\omega)^2+b^2\right)\left(g_\omega+g_\omega^2-b^2\right)^2=b^2g_\omega(2b^2-2g_\omega^2+1). \tag{80}$$

Let g_0 be a limit point for g_ω. There is a sequence $\omega_n \to \infty$ such that $g_n \to g_0$, where g_n stands for the g_ω corresponding to ω_n. From the above relation it follows by dividing with b^2g_n that

$$\begin{aligned}&\frac{b_A^2(\omega_n)}{b^2(\omega_n)}\left((1-g_n)^2+b^2(\omega_n)\right)\left(g_n(1+g_n)^2-2(1+g_n)b^2(\omega_n)+\frac{b^4(\omega_n)}{g_n}\right)\\&=2b^2(\omega_n)-2g_n^2+1\end{aligned} \tag{81}$$

where for clarity we have re-introduced the explicit dependencies on ω. Observe that

$$\lim_{\omega\to\infty}\frac{b_A^2(\omega)}{b^2(\omega)}=\frac{L_F^2}{L_A^2}. \tag{82}$$

We first show that $g_0 > 0$. Assuming the contrary, it would follow by passing to limit into (81) and by taking into account (82) and the fact that, by assumption, $g_n \to 0$,

$$\frac{L_F^2}{L_A^2}\lim_{n\to\infty}\frac{b^4(\omega_n)}{g_n}=1. \tag{83}$$

Consequently,

$$\lim_{n\to\infty}\frac{g_n}{b^2(\omega_n)}=\lim_{n\to\infty}\frac{g_n}{b^4(\omega_n)}b^2(\omega_n)=\frac{L_F^2}{L_A^2}\lim_{n\to\infty}b^2(\omega_n)=0 \tag{84}$$

which contradicts (76).

Since $g_0 > 0$ it now follows that

$$\lim_{n\to\infty}\frac{b^4(\omega_n)}{g_n}=0 \tag{85}$$

and by passing to limit into (81) we obtain that g_0 satisfies (70) with $K=(L_A/L_F)^2$.

Finally it is seen that (70) is converted to (62) by setting $g = 1/r$.

VIII. Conclusions

Starting from the reality that the insertion of a transmission line between a switching power amplifier and a reactive load may introduce unexpected effects manifested as over-amplified higher harmonics in the current through the load, we have presented a computational tool in the form of the peak control function that would help in producing designs immune to the mentioned effects, irrespective of the transmission line length.

We can summarize our achievements and contributions as follows.

a) We have introduced the concepts of biexponential and of simply controlled response functions, for which a lower control and an upper control function could be defined and computed explicitly. The peak control function arose as a particular case of the latter two.

b) We have proved mathematical theorems about the capability of the lower control and of the upper control function to approximate the local extrema of the moduli of the simply controlled functions.

c) The peak control functions for a voltage-mode and a current-mode class D amplifier have been analyzed, and an example circuit has been used for making simulations that were in close agreement with the theoretical calculations.

d) We have computed with the entire mathematical rigor the optimal value of a circuit component according to the criterion established by the peak control function.

In the process we have recognized that the peak control function may explain qualitatively the necessity of the presence of key components at certain places in the circuit and may also establish quantitative criteria for optimization of component values, at least in an asymptotic sense. It would be the task of future research to establish new optimization criteria and algorithms related to the peak control function that would increase even more its utility as a design tool.

References

[1] Y. Cao, “A New Transmitter Circuit for the 13.56MHz RFID Reader Based on ISO14443”, M. S. Thesis, Royal Institute of Technology, Stockholm, 2007.

[2] K. Van Schuylenbergh and R. Puers, Inductive Powering: Basic Theory and Application to Biomedical Systems, pp. 1-15, 112-118, Springer, 2009.

[3] S. D. Keller, "Design and development of directly-modulated antennas using high-speed switching devices", M. S. Thesis, Duke University, 2008.

[4] M. Albulet, RF Power Amplifiers, pp. 131-213, Atlanta, GA: Noble Publishing, 2001.

[5] M. K. Kazimierczuk, RF Power Amplifiers, pp. 109-178, John Wiley & Sons, 2008.

[6] A. Grebennikov, N. O. Sokal and M. J. Franco, Switchmode RF and Microwave Power Amplifiers, 2nd ed., pp. 83-128, Elsevier/Academic Press, 2012.

[7] T. P. Hung, "High Efficiency Switching-mode Amplifiers for Wireless Communication Systems", M. S. Thesis, University of California, San Diego, 2008.

[8] S. A. El-Hamamsy, "Design of High-Efficiency RF Class-D Power Amplifier", IEEE Transactions on Power Electronics, vol. 9, pp. 297–308, May 1994.

[9] H. Kobayashi, J. M. Hinrichs and P. M. Asbeck, "Current-Mode Class-D Power Amplifiers for High-Efficiency RF Applications", IEEE Transactions On Microwave Theory And Techniques, vol. 49, pp. 2480–2485, December 2001.

[10] A. L. Long, "High Frequency Current Mode Class-D Amplifiers With High Output Power and Efficiency", M. S. Thesis, University of California, Santa Barbara, May 2003.

[11] P. Aflaki, R. Negra and F. M. Ghannouchi, "1 GHz Current Mode Class-D Power Amplifier in Hybrid Technology Using GaN HEMTs", Romanian Journal Of Information Science And Technology, vol. 11, pp. 319–328, 2008.

[12] C. H. Kao, P.Y. Tsai, W. P. Lin and Y. J. Chuang, "A switching power amplifier with feedback for improving total harmonic distortion", Analog Integrated Circuits and Signal Processing, vol. 55, pp 205–212, June 2008.

[13] T. Gerrits, J. L. Duarte and M. A. M. Hendrix, "Third Harmonic Filtered 13.56 MHz Push-Pull Class-E Power Amplifier", in Proceedings of the 2010 IEEE Energy Conversion Congress and Exposition (ECCE), pp. 742–749, September 2010.

[14] J. Fritzin, C. Svensson and A. Alvandpour, "A Class-D outphasing RF amplifier with harmonic suppression in 90nm CMOS", in Proceedings of the ESSCIRC 2010 Conference, pp. 310–313, September 2010.

[15] J. Fritzin, C. Svensson and A. Alvandpour, "Design and Analysis of a Class-D Stage with Harmonic Suppression", IEEE Transactions on Circuits and Systems I, vol. 59, pp. 1178–1186, June 2012.

[16] A. Shirvani and B. A. Wooley, Design and Control of RF Power Amplifiers, pp. 66-67, Kluwer Academic Press, 2003.

[17] Belden, "7805 Coax - RG-174 Type, Detailed Specifications and Technical Data". [Online]. Available: http://www.belden.com/techdatas/metric/7805.pdf

[18] D. T. Vuza, R. Frosch and M. Vlădescu, "Transmission line effects in Class D amplifiers – The peak control function as a design tool", in Proceedings of the IEEE 18th International Symposium for Design and Technology of Electronics Packages (SIITME), pp. 53–58, Alba Iulia, October 2012.

[19] G. E. Shilov, Elementary Real and Complex Analysis, Dover Publications, Inc., New York 1973.

[20] D. M. Pozar, Microwave Engineering, 3rd ed., pp. 49-63, John Wiley & Sons, 2005.